Method of Moments (MoM) Modeling of Wave Propagation Inside a Wedge Waveguide

G. Apaydin [1] and L. Sevgi [2]

[1] Department of Electrical-Electronics Engineering
Zirve University, Gaziantep, 27260, Turkey
gokhan.apaydin@zirve.edu.tr

[2] Department of Electrical-Electronics Engineering
Işık University, Faculty of Engineering, Şile/Istanbul, 34980, Turkey
ls@leventsevgi.net

Abstract ─ Method of Moments (MoM) is used to model guided wave propagation inside a non-penetrable wedge waveguide and the results are validated against analytical mode-based exact solutions.

Index Terms ─ Adiabatic modes, electromagnetic propagation, Green's function, guided waves, intrinsic modes, Method of Moments (MoM), modeling, normal modes, simulation, waveguide, wedge.

I. INTRODUCTION

Natural or man-made guiding environments are usually characterized by physical parameters that render the wave equation non-separable in any of the standard coordinate systems [1-2]. If separable, transverse and longitudinal decomposition of wave equation yields Normal Modes (NM) [1]. NMs are the solutions of source-free wave equation, individually satisfy the transverse Boundary Conditions (BC), and propagate longitudinally without coupling to other modes. When transverse-longitudinal separability is only weakly perturbed, Adiabatic (local) Modes (AM) can be used [3-5]. AMs adapt smoothly without intermode coupling, to the slowly changing conditions, but fail in cut-off regions. This failure can be uniformized by Intrinsic Modes (IM) [6-8]. These concepts can best be explained by investigating the wave dynamics in a simple test environment: a wedge waveguide with non-penetrable boundaries. Source-driven solutions may then be obtained via Green's function (i.e., line-source response) based on these modes. Alternatively, pure numerical methods can be used to investigate wave propagation inside a wedge waveguide with non-penetrable boundaries.

Wedge with non-penetrable (i.e., Perfectly Electrical Conductor, PEC) boundaries is a canonical structure where analytical as well as numerical models are derived, tested, and validated. It is also used to gain physical insight. Wedge with an exterior source serves as reference for understanding and solving the scattering phenomena [9-11]. Wedge scattering may also be modeled with numerical models, such as the Finite-Difference Time-Domain (FDTD) [12,13] or Method of Moments (MoM) [14-18].

Wedge with an interior source is canonical in understanding and solving guided wave phenomena using both analytical and numerical models. The Green's function of this problem can be extracted using both mode summation and ray-tracing/eigenray extraction models (see, [19,20] for tutorial reviews and free MATLAB-based virtual tools).

In this study, propagation inside a wedge waveguide with PEC boundaries is modeled using MoM and validated against analytical exact solutions. The paper is organized as follows. In Section II, guided waves inside a wedge-type waveguide are summarized for the sake of completeness. MoM solutions of guided waves excited by a line source are given in Section III. Section IV contains numerical comparisons of

Submitted On: March 15, 2014
Accepted On: August 10, 2014

Green's function and MoM solutions. Finally, the conclusions are presented in Section V.

II. GUIDED WAVES: GREEN'S FUNCTION SOLUTION

The two-dimensional wedge waveguide with apex angle (α) is pictured in Fig. 1. Here, *x* and *y* are the longitudinal (range) and transverse (height above *y*=0) coordinates, respectively. The structure is infinite along *z*-direction ($\partial/\partial z \equiv 0$). Note, that the problem is separable in cylindrical coordinates (ρ,φ) and exact solution can be built in terms of infinite mode summation. On the other hand, visualization is better in rectangular coordinates (x,y). Therefore, both coordinate systems are used in this paper.

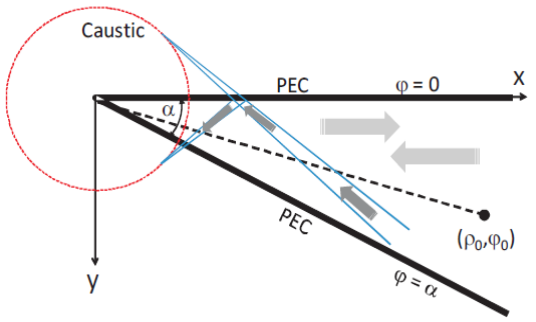

Fig. 1. Geometry of the wedge waveguide problem.

Under the time dependence $\exp(-i\omega t)$, the Green's function of this problem is postulated via:

$$\left\{\frac{1}{\rho}\frac{\partial}{\partial\rho}\left(\rho\frac{\partial}{\partial\rho}\right)+\frac{1}{\rho^2}\frac{\partial^2}{\partial\phi^2}+k^2\right\}u_{s,h}=\frac{I_0}{\rho}\delta(\rho-\rho_0)\delta(\phi-\phi_0), \quad (1)$$

where $k=2\pi/\lambda=\omega\sqrt{\varepsilon_0\mu_0}$ is the free-space wave-number, I_0 is the line current amplitude, (ρ_0,φ_0) and (ρ,φ) specify the source and the observation points, respectively, $\delta(\cdot)$ is the Dirac delta functions. In the case of Electromagnetic (EM) waves, the BCs are appropriate for the PEC wedge and u_s represents the *z*-component of electric field intensity E_z (TM), while u_h is the *z*-component of magnetic field intensity H_z (TE). In the case of acoustic waves, these conditions refer to acoustically soft (TM $\rightarrow$ SBC) and hard (TE $\rightarrow$ HBC) wedges, respectively. Mathematically, they are Dirichlet and Neumann BCs, respectively. Note, that the Green's function notation $u_{s,h}=g_{s,h}(\rho,\varphi,\rho_0,\varphi_0)$ is used here.

The Green's function solution is exact in polar coordinates but requires infinite number of mode summation. The wave equation inside the wedge illuminated by a line source is subject to the BC:

$$u_s=0 \text{ or } \partial u_h/\partial n=0 \text{ on } \varphi=0,\alpha, \quad (2)$$

satisfy *radiation condition* for $\rho\rightarrow\infty$, and *finiteness* at $\rho\rightarrow 0$. Two different propagation scenarios are possible in this wedge waveguide problem. One of them is downslope propagation where the source is close to the apex ($\rho\geq\rho_0$). In this case, one-way propagation is of interest; waves excited by the source travel downslope without any back-reflections. The interesting case is the upslope propagation ($\rho_0\geq\rho$), as shown in Fig. 1, where the wave fields travel in the direction of narrowing waveguide cross-section up to the cut-off (caustic) transition region, converting the incoming waves into reflected and evanescent fields on the propagating and non-propagating sides, respectively, of the caustic.

Waves excited by any given source can be represented in terms of mode and/or ray summation [19]. NMs propagating upslope towards the tip, reaching their propagating-to-evanescent cutoff transition point and totally reflect back. Their interaction yield standing waves before the cut-off range. On the other hand, they exponentially decay beyond their modal cut-off ranges (also called turning point) (see, Fig. 2). In terms of rays, upslope going rays bounce back and forth between two boundaries and their angles of reflection increase each time they bounce. Rays totally go back once their reflection angles reach 90°. These occur at modal cut-off ranges.

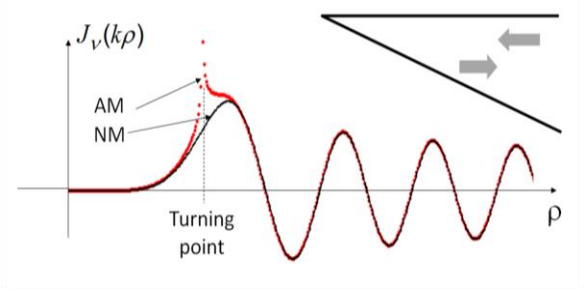

Fig. 2. Longitudinal variation of a single mode.

The exact total fields in polar coordinates

using Green's function with SBC and HBC are [1]:

$$u_s = \begin{cases} \frac{\pi}{i\alpha} I_0 \sum_{l=1}^{\infty} J_{\nu_l}(k\rho) H_{\nu_l}^{(1)}(k\rho_0) \sin(\nu_l \varphi_0) \sin(\nu_l \varphi), & \rho \le \rho_0 \\ \frac{\pi}{i\alpha} I_0 \sum_{l=1}^{\infty} J_{\nu_l}(k\rho_0) H_{\nu_l}^{(1)}(k\rho) \sin(\nu_l \varphi_0) \sin(\nu_l \varphi), & \rho \ge \rho_0 \end{cases}, \quad (3a)$$

$$u_h = \begin{cases} \frac{\pi}{i\alpha} I_0 \sum_{l=0}^{\infty} \varepsilon_l J_{\nu_l}(k\rho) H_{\nu_l}^{(1)}(k\rho_0) \cos(\nu_l \varphi_0) \cos(\nu_l \varphi), & \rho \le \rho_0 \\ \frac{\pi}{i\alpha} I_0 \sum_{l=0}^{\infty} \varepsilon_l J_{\nu_l}(k\rho_0) H_{\nu_l}^{(1)}(k\rho) \cos(\nu_l \varphi_0) \cos(\nu_l \varphi), & \rho \ge \rho_0 \end{cases}. \quad (3b)$$

Here, $\nu_l = l\pi/\alpha$, $\varepsilon_0 = 0.5$, $\varepsilon_1 = \varepsilon_2 = \varepsilon_3 = \cdots = 1$.

The solution (3) is exact and valid for all wedge angles. Infinite modes are required in representing a line source near the source region, but only propagating modes are enough in the far field. As the wedge angle increases, the number of propagating modes for the same parameters increases (see, Table 1); therefore, computations in terms of the exact solution take longer. This also determines the accuracy. One needs to take into account a certain number of modes in the near field in order to satisfy given accuracy. The source and observer locations determine the excited modes. One can eliminate even or odd modes by locating source or observer accordingly. Locating the line source near a boundary does only affect the number of excited modes.

Table 1: The number of propagating modes vs. wedge angle ($x = 60\,\text{m}$, $f = 15\,\text{MHz}$, source location; $\rho_0 = 600\,\text{m}$, $\varphi_0 = 1.5°$, polarization: horizontal)

Apex Angle α [deg]	# Of Propagating Modes
3	5
15	24
30	49

III. MOM SOLUTION OF GUIDED WAVES

Method of Moments (MoM) is one of the oldest and most effective numerical EM technique in frequency domain for problems that cannot be *exactly* solved [14]. It has long been applied to scattering problems [15]. Propagation inside resonating structures may also be modeled with MoM [16,17]. It has recently been illustrated that MoM accurately accounts for the wedge diffracted fields and fringe waves [18].

Propagation inside a wedge waveguide with non-penetrable boundaries may also be modeled by using MoM. In this model, the faces of the wedge are divided into small segments (see, Fig. 3). N segments for the top face at $\varphi = 0$ and N segments for the bottom face at $\varphi = \alpha$ are used. The segment lengths are very small compared to the wavelength so that the line-source-induced currents on each segment may be assumed constant.

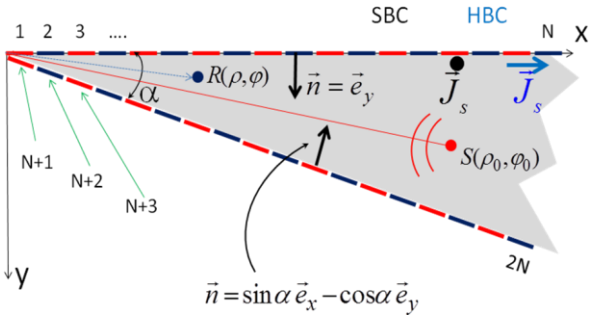

Fig. 3. Wedge waveguide and MoM modeling.

Necessary MoM equations in this procedure are formed with the source excited incident fields on BC:

$$V_n = -E_z^{inc}(\boldsymbol{\rho}_\mathbf{n}) = H_0^{(1)}(kd_n)/(4i) \quad \text{(SBC)}, \quad (4a)$$

$$V_n = -H_z^{inc}(\boldsymbol{\rho}_\mathbf{n}) = H_0^{(1)}(kd_n)/(4i) \quad \text{(HBC)}, \quad (4b)$$

by using distance (d_n) between line source and each segment,

$$d_n = \sqrt{[x(\boldsymbol{\rho}_\mathbf{n}) - x_0]^2 + [y(\boldsymbol{\rho}_\mathbf{n}) - y_0)]^2}, \quad (5)$$

where $x_0 = \rho_0 \cos\varphi_0$, $y_0 = \rho_0 \sin\varphi_0$. The impedance matrix is obtained:

$$Z_{nm} \cong \begin{cases} -\frac{k\eta_0 \Delta l}{4} H_0^{(1)}\left(k|\boldsymbol{\rho}_\mathbf{n} - \boldsymbol{\rho}_\mathbf{m}|\right), & m \ne n \\ -\frac{k\eta_0 \Delta l}{4}\left[1 + i\frac{2}{\pi}\log\left(\frac{\gamma k \Delta l}{4e}\right)\right], & m = n \end{cases} \quad \text{(SBC)}, \quad (6a)$$

$$Z_{nm} \cong \begin{cases} \frac{-ik\Delta l}{4} H_1^{(1)}\left(k|\boldsymbol{\rho}_\mathbf{n} - \boldsymbol{\rho}_\mathbf{m}|\right)(\hat{\mathbf{n}}_\mathbf{m} \cdot \hat{\boldsymbol{\rho}}_{\mathbf{mn}}), & m \ne n \\ 0.5, & m = n \end{cases} \quad \text{(HBC)}, \quad (6b)$$

where Δl is the segment length, $\eta_0 \approx 120\pi$ is the intrinsic impedance of free space, $H_0^{(1)}$ and $H_1^{(1)}$ are the first kind Hankel functions with order zero and one, respectively, $\gamma \approx 1.781$ is the exponential of the Euler constant, $\hat{\mathbf{n}}_\mathbf{m}$ denotes the unit normal vector of the segment at $\boldsymbol{\rho}_\mathbf{m}$, and $\hat{\boldsymbol{\rho}}_{\mathbf{mn}}$ is the unit vector in the direction from source $\boldsymbol{\rho}_\mathbf{m}$ to the receiving element $\boldsymbol{\rho}_\mathbf{n}$.

First, the source-excited segment fields are calculated by using the two-dimensional free-space Green's function (4). Then, the impedance matrix is formed by (6). The unknown segment currents are derived by the solution of $2N\times 2N$ matrix system $[I]=[Z]^{-1}[V]$. Once they are calculated, the scattered fields at the observer are obtained as:

$$E_z^{sct}(\boldsymbol{\rho}_\mathbf{n}) \cong -\frac{k\eta_0 \Delta l}{4}\sum_{m=1}^{2N} I_m H_0^{(1)}\left(k|\boldsymbol{\rho}_\mathbf{n}-\boldsymbol{\rho}_\mathbf{m}|\right), \quad (7a)$$

$$H_z^{sct}(\boldsymbol{\rho}_\mathbf{n}) \cong -\frac{ik\Delta l}{4}\sum_{m=1}^{2N} I_m H_1^{(1)}(k|\boldsymbol{\rho}_\mathbf{n}-\boldsymbol{\rho}_\mathbf{m}|)(\hat{\mathbf{n}}_\mathbf{m}\cdot\hat{\boldsymbol{\rho}}_\mathbf{mn}), \quad (7b)$$

and the segment-scattered fields at the observer are accumulated. Finally, the direct wave from the source to the observer is added and the total fields are obtained.

IV. NUMERICAL EXAMPLES AND COMPARISONS

Waves inside a non-penetrable wedge waveguide obtained with the Green's function and MoM approaches are compared in this section. Both models are run with various scenarios under different sets of parameters. A few results are presented in Figs. 4-10. Infinite wedge faces are truncated in 100λ and the segment lengths are chosen λ/20 (i.e., total of 4000 segments on both faces which necessitate the solution of 4000 by 4000 system of equations). Note, that the finite length of the wedge faces must extend several dozen wavelengths beyond the source and the observer on both sides; therefore, the number of segments may significantly differ. As observed, very good agreement is obtained between analytical and numerical models.

Field vs. radial range at mid-angle ($\varphi = 7.5°$) inside a $\alpha = 15°$ wedge waveguide obtained with the analytical and numerical models is shown in Fig. 4. The frequency is 15 MHz. Horizontal polarization (TM/SBC case) is taken into account. The source location is at $\rho_0 = 500\,\text{m}$ and $\varphi_0 = 7.5°$. The first three modal cutoff ranges obtained from $\rho_l = 0.5l\lambda/\alpha$ are 38.2 m, 76.4 m, and 114.6 m. As observed, propagation-to-evanescent cut-off transition ranges of the first and third modes at 38.2 m and 114.6 m are visible, but the second mode at 76.4 m is invisible. This is merely because of the location of the source in this example. Only odd-order modes are excited if the source is located at mid-angle, which is the null-angle for these modes. As observed, the agreement between the two models is almost perfect even for these highly oscillatory variations.

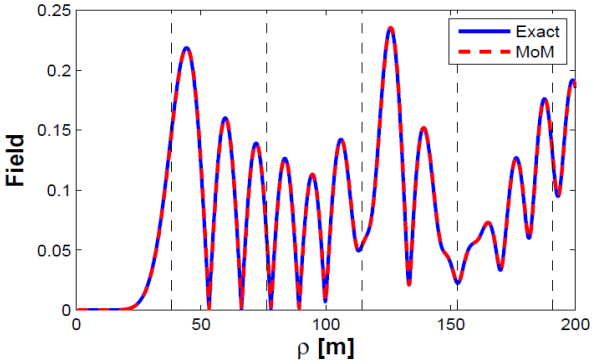

Fig. 4. Field vs. radial range at mid-angle inside the wedge; solid: Green's function, dashed: MoM (TM/SBC case, $\alpha = 15°$, $f = 15\,\text{MHz}$, $\rho_0 = 500\,\text{m}$).

Field vs. height inside the same wedge waveguide at three different ranges is plotted in Fig. 5. These are the ranges with only one, two, and three propagating modes, respectively. Note, that these are not angular variations and the height is along *y*-direction. On the left, only the dominant mode is shown. At the given range in the middle, two modes are propagating. On the right, there are three propagating modes, but only two of them are excited.

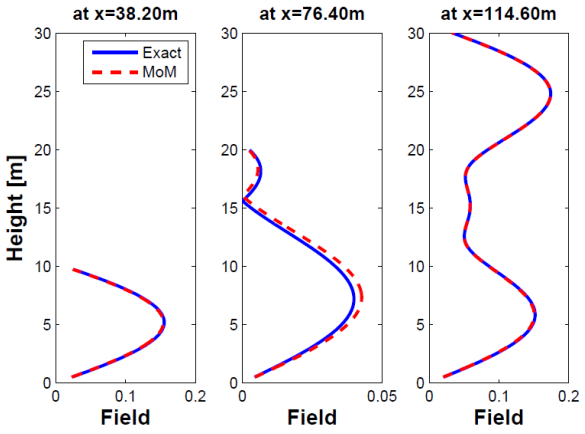

Fig. 5. Field vs. height (along *y*) inside the wedge at three different ranges; solid: Green's function, dashed: MoM (SBC case, $\alpha = 15°$, $f = 15\,\text{MHz}$, $\rho_0 = 500\,\text{m}$).

The other two examples plotted in Figs. 6 and 7 belong to the same wedge waveguide but for different polarizations. Field vs. height at 900 m inside the same wedge waveguide for both TM and TE polarizations are plotted in Fig. 6. The line source is at $x_0 = 1000\,\text{m}$ and $y_0 = 135\,\text{m}$. For the same source location, field vs. range (along *x*-direction) at 110 m inside the same wedge waveguide for both TM and TE polarizations are plotted in Fig. 7. As observed, the agreement between two models is impressive.

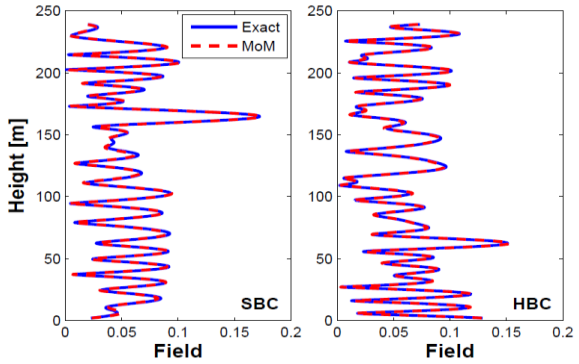

Fig. 6. Field vs. height (along y at $x = 900\,\text{m}$ range) inside the wedge; solid: MoM, dashed: Green's function (Left) TM/SBC case, (Right) TE/HBC case ($\alpha = 15°$, $f = 15\,\text{MHz}$, $x_0 = 1000\,\text{m}$, $y_0 = 135\,\text{m}$).

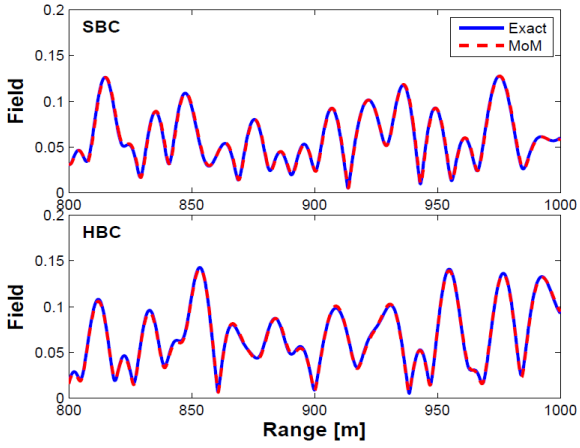

Fig. 7. Field vs. range (along x at $y = 110\,\text{m}$ height) inside the wedge; solid: MoM, dashed: Green's function (Top) TM/SBC case, (Bottom) TE/HBC case ($\alpha = 15°$, $f = 15\,\text{MHz}$, $x_0 = 1000\,\text{m}$, $y_0 = 135\,\text{m}$).

The next two examples plotted in Figs. 8 and 9 belong to a wider wedge waveguide at the same frequency for different polarizations. Field vs. height at 300 m inside the same wedge waveguide for both TM and TE polarizations are plotted in Fig. 8. The line source is at $x_0 = 500$ m and $y_0 = 15$ m. For the same source location, field vs. range at 10 m inside the same wedge waveguide for both TM and TE polarizations are plotted in Fig. 9.

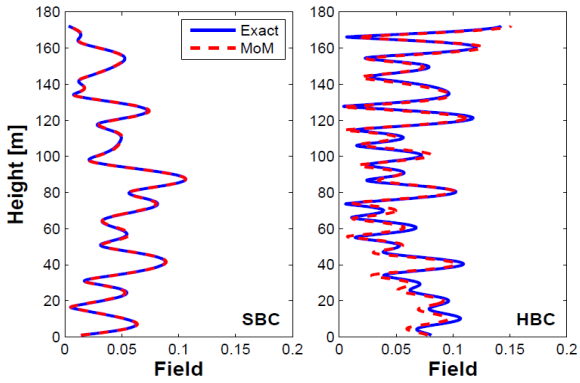

Fig. 8. Field vs. height (along y at 300 m range) inside the wedge; solid: MoM, dashed: Green's function (Left) TM/SBC case, (Right) TE/HBC case ($\alpha = 30°$, $f = 15\,\text{MHz}$, $x_0 = 500\,\text{m}$, $y_0 = 15\,\text{m}$).

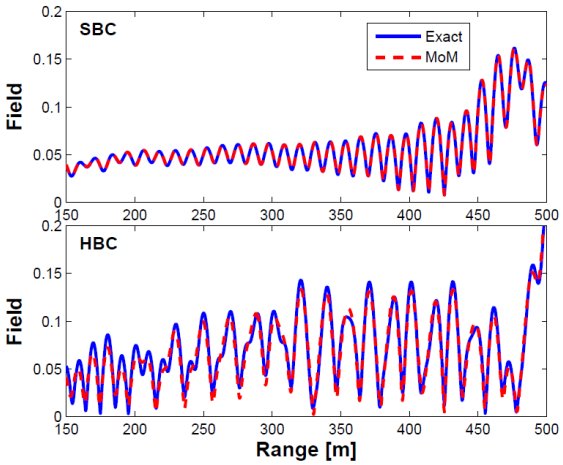

Fig. 9. Field vs. range (along x at y=10 m height) inside the wedge; solid: MoM, dashed: Green's function (Top) TM/SBC case, (Bottom) TE/HBC case ($\alpha = 30°$, $f = 15\,\text{MHz}$, $x_0 = 500\,\text{m}$, $y_0 = 15\,\text{m}$).

Note, that two MatLab algorithms are developed and computations are performed. A kind of accuracy test is used in both Green's function and MoM algorithms. Both propagating and evanescent modes are taken into account in the analytic model. The contribution of each mode is controlled and higher order modes with contributions less than 10^{-12} are neglected. In MoM, the number of segments per wavelength is tested once and optimum segmentation is specified.

Table 2 shows the result of this test using relative L2-error norm:

$$error = 100 \times \frac{\|u_A - u_N\|}{\|u_A\|}, \qquad (8)$$

where u_A is the analytical result, u_N is the numerical result. As observed, HBC polarization needs more segments.

Table 2: Relative L2-*error* norm analysis at $y = 3\,\text{m}$, 1000 points are used between *x*=20 m and *x*=250 m,($\alpha = 15°$, $f = 15\,\text{MHz}$. Source: $x_0 = 250\,\text{m}$, $y_0 = 33\,\text{m}$)

Segment Length (m)	Error % (SBC)	Error % (HBC)
λ/10	10.22	22.85
λ/20	5.36	10.79
λ/40	2.69	6.12
λ/80	1.32	3.98

The last example belongs to three dimensional comparisons. Figure 10 shows field vs. range/height as three dimensional color-plots. The dashed arcs show modal cut-offs. A line source is located at mid-angle of a 20° non-penetrable wedge. The exact location of the source is $x_0 = 200\,\text{m}$, $y_0 = 32.26\,\text{m}$. The frequency is 15 MHz. The number of propagating modes at the source distance is 7. Not only the odd-numbered modes are excited with this source location but also the transverse interference is observed for the downslope/one-way propagation (i.e., for the observer ranges greater than 200 m). On the other hand, both the transverse and the longitudinal interaction is observed for upslope/two-way propagation (i.e., for the observer distance less than 200 m). As observed, very good agreement is obtained in this example, too.

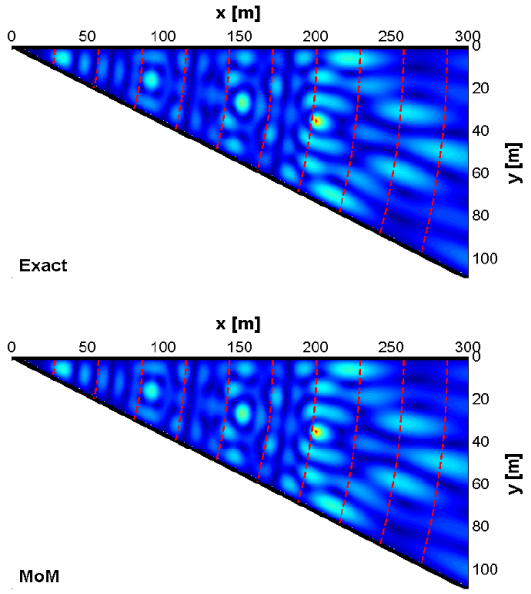

Fig. 10. The three dimensional color plots of field vs. range-height variations inside the wedge waveguide: (Top) Exact, (Bottom) MoM, TM/SBC case, ($\alpha = 20°$, $f = 15\,\text{MHz}$, $x_0 = 200\,\text{m}$, $y_0 = 32.26\,\text{m}$, $\Delta l = \lambda/20$, $\Delta x = 1\,\text{m}$, $\Delta y = 1\,\text{m}$).

V. CONCLUSION

A Method of Moments (MoM) based procedure is introduced for the simulation of guided waves excited by a line source inside the wedge with perfectly conducting boundaries. Tests and comparisons are performed against the Green's function solution based on Normal Mode (NM) summation. The results show that MoM is also successful in accurate modeling of guided waves inside wedge waveguide.

REFERENCES

[1] L. B. Felsen and N. Marcuvitz, "Radiation and scattering of waves," *Prentice-Hall*, New Jersey, 1973. *Classic reissue by IEEE Press*, Piscataway, New Jersey, 1994.

[2] G. Dudley, "Mathematical foundations for electromagnetic theory," *IEEE Press (Series on Electromagnetic Waves)*, New York, 1994.

[3] A. D. Pierce, "Extension of the method of normal modes to sound propagation in almost stratified medium," *J. Acoust. Soc. Am.*, vol. 37, pp. 19-27, 1965.

[4] L. B. Felsen and L. Sevgi, "Adiabatic and intrinsic modes for wave propagation in guiding environments with longitudinal and transverse

variations: formulation and canonical test," *IEEE Trans. Antennas Propagat*., vol. 39, no. 8, pp. 1130-1136, August 1991.

[5] L. B. Felsen and L. Sevgi, "Adiabatic and intrinsic modes for wave propagation in guiding environments with longitudinal and transverse variations: continuously refracting media," *IEEE Trans. Antennas Propagat*., vol. 39, no. 8, pp. 1137-1143, August 1991.

[6] L. Sevgi, "Local intrinsic modes: a new method to solve non-separable wave problems," Ph.D. Dissertation, *ITU Institute of Science*, Istanbul, 1990.

[7] E. Topuz and L. Sevgi, "Intrinsic mode representations of the green's functions for a benchmark problem: the non-penetrable wedge," *Journal of Electromagnetic Waves and Applications*, vol. 9, no. 7/8, pp. 1065-1082, 1995.

[8] E. Topuz and L. B. Felsen, "Intrinsic modes: numerical implementation in a wedge-shaped ocean," *J. Acoust. Soc. Am.*, vol. 88, pp. 1735-1745, 1985.

[9] C. Balanis, L. Sevgi, and P. Ya Ufimtsev, "Fifty years of high frequency asymptotics," *International Journal on RF and Microwave Computer-Aided Engineering*, vol. 23, no. 4, pp. 394-402, July 2013.

[10] F. Hacivelioglu, L. Sevgi, and P. Ya. Ufimtsev, "Electromagnetic wave scattering from a wedge with perfectly reflecting boundaries: analysis of asymptotic techniques," *IEEE Antennas and Propagation Magazine*, vol. 53, no. 3, pp. 232-253, June 2011.

[11] F. Hacivelioglu, L. Sevgi, and P. Ya. Ufimtsev, "Wedge diffracted waves excited by a line source: exact and asymptotic forms of fringe waves," *IEEE Trans. Antennas Propagat*., vol. 61, no. 9, pp. 4705-4712, 2013.

[12] G. Cakir, L. Sevgi, and P. Ya. Ufimtsev, "FDTD modeling of electromagnetic wave scattering from a wedge with perfectly reflecting boundaries: comparisons against analytical models and calibration," *IEEE Trans. Antennas Propagat*., vol. 60, no. 7, pp. 3336-3342, July 2012.

[13] M. A. Uslu and L. Sevgi, "Matlab-based virtual wedge scattering tool for the comparison of high frequency asymptotics and FDTD method," *Int. Journal on Applied Computational Electromagnetics*, vol. 27, no. 9, pp. 697-705, September 2012.

[14] R. F. Harrington, "Field computation by moment method," *New York: IEEE Press*, (first ed. 1968), 1993.

[15] E. Arvas and L. Sevgi, "A tutorial on the method of moments," *IEEE Antennas and Propagation Magazine*, vol. 54, no. 3, pp. 260-275, June 2012.

[16] G. Apaydin and L. Sevgi, "A canonical test problem for computational electromagnetics (cem): propagation in a parallel-plate waveguide," *IEEE Antennas and Propagation Magazine*, vol. 54, no. 4, pp. 290-315, 2012.

[17] G. Apaydin and L. Sevgi, "Method of moment (MoM) modeling for resonating structures: propagation inside a parallel plate waveguide," *Int. Journal on Applied Computational Electromagnetics*, vol. 27, no. 10, pp. 842-849, October 2012.

[18] G. Apaydin, F. Hacivelioglu, L. Sevgi, and P. Ya. Ufimtsev, "Wedge diffracted waves excited by a line source: method of moments (MoM) modeling of fringe waves," *IEEE Trans. Antennas Propagat*., vol. 62, no. 8, pp. 4368-4371, August 2014.

[19] L. Sevgi, F. Akleman, and L. B. Felsen, "Visualizations of wave dynamics in a wedge-waveguide with non-penetrable boundaries: normal, adiabatic, and intrinsic mode representations," *IEEE Antennas and Propagation Magazine*, vol. 49, no. 3, pp. 76-94, June 2007.

[20] L. B. Felsen, F. Akleman, and L. Sevgi, "Wave propagation inside a two-dimensional perfectly conducting parallel-plate waveguide: hybrid ray-mode techniques and their visualizations," *IEEE Antennas and Propagation Magazine*, vol. 46, no. 6, pp. 69-89, December 2004.

Gökhan Apaydin received his B.S., M.S., and Ph.D. degrees in Electrical and Electronics Engineering from Bogazici University, Istanbul, Turkey, in 2001, 2003, and 2007, respectively. From 2001 to 2005, he was a Teaching and Research Assistant with Bogazici University. From 2005 to 2010, he was a Project and Research Engineer with Applied Research and Development, University of Technology Zurich, Zurich, Switzerland. Since 2010, he has been with Zirve University, Gaziantep, Turkey. He has been working on several research projects on analytical and numerical methods (FEM, MoM, FDTD, SSPE) in electromagnetic propagation, radiowave propagation modeling, diffraction modeling, positioning, filter design, waveguides, and related areas.

Levent Sevgi received his Ph.D. degree from Istanbul Technical University, Istanbul, Turkey, and Polytechnic Institute of New York University, Brooklyn, in 1990. Professor Leo Felsen was his advisor. He was with Istanbul Technical University from 1991 to 1998; TUBITAK-MRC, Information Technologies Research Institute, Gebze/Kocaeli, Turkey, from 1999 to 2000; Weber Research Institute/Polytechnic University of New York, from 1988 to 1990; Scientific Research Group of Raytheon Systems, Canada, from 1998 to 1999; and the Center for Defense Studies, ITUVSAM, from 1993 to 1998 and from 2000 to 2002, Doğuş University from 2001 to 2014. He was with the Massachusetts University as a Visiting Professor from September 2012 to July 2013, during his sabbatical term. He has been with Işık University, Istanbul since September 2014. He has been involved with complex Electromagnetic (EM) problems and systems for more than two decades.

He is the author of the books entitled *Complex Electromagnetic Problems and Numerical Simulation Approaches* (2003), and *Electromagnetic Modeling and Simulation* (2014), published by the IEEE Press and John Wiley.

Sevgi is an IEEE Fellow, the Writer/Editor of the "Testing Ourselves" Column in the IEEE Antennas and Propagation Magazine and a member of the IEEE AP-S Education Committee.